BIOCHEMISTRY
including biophysical chemistry & molecular biology
Article

Biochemistry **2010,** *49,* 6541–6549 6541
DOI: 10.1021/bi100793y

Regulation of β-Lactamase Activity by Remote Binding of Heme: Functional Coupling of Unrelated Proteins through Domain Insertion†

Wayne R. Edwards,‡,§ Abigail J. Williams,‡ Josephine L. Morris,‡,§ Amy J. Baldwin,‡,§ Rudolf K. Allemann,§ and D. Dafydd Jones*,‡

‡*School of Biosciences and* §*School of Chemistry, Cardiff University, Cardiff, U.K.*

Received May 19, 2010; Revised Manuscript Received June 25, 2010

ABSTRACT: Coupling the activities of normally disparate proteins into one functional unit has significant potential in terms of constructing novel switching components for synthetic biology or as biosensors. It also provides a means of investigating the basis behind transmission of conformation events between remote sites that is integral to many biological processes, including allostery. Here we describe how the structures and functions of two normally unlinked proteins, namely, the heme binding capability of cytochrome b_{562} and the antibiotic degrading β-lactamase activity of TEM, have been coupled using a directed evolution domain insertion approach. The important small biomolecule heme directly modulates in vivo and in vitro the β-lactamase activity of selected integral fusion proteins. The presence of heme decreased the concentration of ampicillin tolerated by *Escherichia coli* and the level of in vitro hydrolysis of nitrocefin by up to 2 orders of magnitude. Variants with the largest switching magnitudes contained insertions at second-shell sites that abut key catalytic residues. Spectrophotometry confirmed that heme bound to the integral fusion proteins in a manner similar to that of cytochrome b_{562}. Circular dichroism suggested that only subtle structural changes rather than gross folding−unfolding events were responsible for modulating β-lactamase activity, and size exclusion chromatography confirmed that the integral fusion proteins remained monomeric in both the apo and holo forms. Thus, by sampling a variety of insertion positions and linker sequences, we are able to couple the functions of two unrelated proteins by domain insertion.

The ability to construct tailored artificial protein switches that control specific biological processes is integral to synthetic biology (*1*−*3*), as it opens up the possibility of generating novel biomolecular components that can act as regulators or sensors. Furthermore, it provides an opportunity to test our understanding of how events at sites distant from each other communicate through coupled conformation events, which is an essential feature of many naturally occurring protein switches (*4*). One strategy for constructing such protein switches is based on the concept of allostery (*4*, *5*), whereby a remote regulatory site can modulate activity in either a negative or positive fashion; regulation is achieved through conformational or dynamical changes occurring at the regulatory site being propagated through to the active site. Allosteric proteins are common in nature and are often involved in regulating metabolic and signal transduction pathways (*5*, *6*).

To construct artificial protein switches that mimic allostery, a strategy called domain insertion can be employed (*7*−*9*). Domain insertion is a process by which integral fusion proteins are constructed through the placement of one protein domain (the "insert") within the sequence of a second (the "parent"). Tolerance of the insert domain within the folded structure of the parent will introduce greater connectivity between the domains, which can potentially generate interdependence between the two proteins at the structural and functional level. For example, ligand-induced structural changes to a sensing domain can be utilized to influence the output of a reporter domain, thereby introducing a switching function into the hybrid protein (Figure 1A). There is a requirement for the N- and C-termini of the insert protein to be close in space to each other, but given that ∼50% of proteins in the Protein Data Bank (PDB)[1] are proximal (*10*), many proteins should be open to this strategy.

Domain insertion by rational protein engineering has had only limited success (*11*−*13*). Even when using advanced computational approaches (*14*), it is still difficult to predict a site tolerant to domain insertion that will also result in significant coupling of individual protein domains. This is further complicated by the nature of the linking sequence that connects the two domains: too short and domain insertion may not be tolerated, too long and the separate functionalities may be uncoupled. A more robust strategy is generation of libraries (*15*, *16*) that randomly sample a number of insertion positions and linking sequences that connect the two domains. This approach will not only improve the engineering of new protein scaffolds with inherent switching but also allow a retrospective analysis of how communication between two distinct sides can be achieved. To this end, a transposon-based random nonhomologous recombination method was developed (*15*, *17*). Using this approach, a novel biological system was constructed in which the important biomolecule heme (*18*) was used to regulate bacterial antibiotic

†This work was supported by the BBSRC (BB/E007384 and BB/E001084) and the Welsh Assembly Government (HE07POC3007).

*To whom correspondence should be addressed: School of Biosciences, Main Building, Cardiff University, Cardiff CF10 3AT, U.K. E-mail: jonesdd@cf.ac.uk. Telephone: +44 (0)2920874290. Fax: +44 (0)2920874305.

[1]Abbreviations: CD, circular dichroism; cyt *b*, cytochrome b_{562}; MIC, minimum inhibitory concentration; SEC, size exclusion chromatography; PDB, Protein Data Bank.

Published on Web 07/05/2010

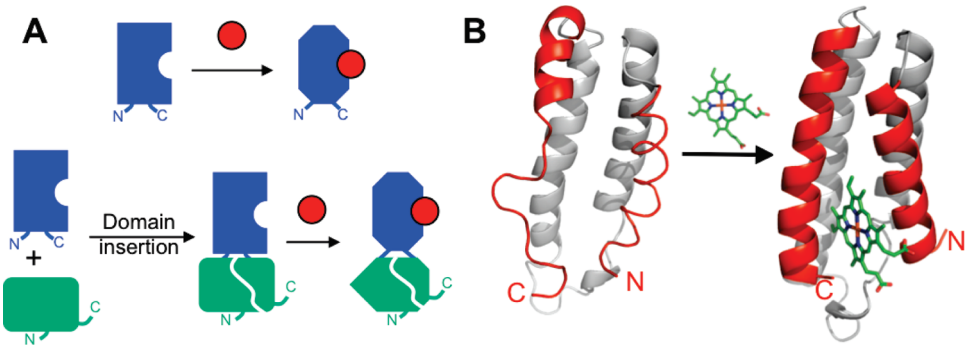

FIGURE 1: Domain insertion as a strategy for coupling the activities of two unrelated proteins. (A) Outline of the domain insertion strategy. A sensing protein (blue) undergoes a conformational change in response to a stimulus (red circle) such as a small molecule. The insertion of the sensing protein within another unrelated reporter protein (green) can intimately link the structure of the two proteins such that events in the sensing domain on stimulus recognition can be transmitted to and thus regulate the activity of the reporter protein. (B) Structural changes to apo-cyt *b* [PDB entry 1apc (*24*)] upon binding of heme [PDB entry 1qpu (*21*)].

resistance by linking the normally unrelated proteins cytochrome b_{562} (cyt *b*) and TEM β-lactamase (*15*). Heme is an essential cofactor for many different proteins that have roles ranging from transport to catalysis to regulation of gene expression (*19*, *20*). Thus, sensing heme and its availability in biological systems is important.

Cyt *b* is a heme binding protein found in the periplasm of *Escherichia coli* and has been the subject of extensive structure, folding, and protein engineering studies (*21*−*29*). This four-helix bundle protein binds heme noncovalently close to the termini through two ligands that coordinate to the heme iron moiety, a methionine at position 7 and a histidine at position 102. Heme binding induces a major change in the structural and dynamics of the protein (Figure 1B). The most notable occurs in the fourth helix, which changes from dynamic structure to a helix locked into its conformation by coordination of His102 to the heme iron (*22*, *24*). This in turns alters the spatial positioning and dynamics of the N- and C-termini with respect to each other (Figure 1B), which provides a mechanism for transferring conformational events on heme recognition to a second, reporter protein. TEM is a class A serine β-lactamase (*30*) that confers bacterial resistance to a variety of β-lactam antibiotics through cleavage of the amide bond in the β-lactam ring (*30*). Therefore, TEM represents a useful reporter protein both in vivo and in vitro.

Here we provide a direct investigation of several cyt *b*−TEM integral fusion proteins selected from a library of variants tolerant to the insertion of cyt *b* at various different positions within TEM. The selected cyt *b*−TEM integral fusion variants imposed a heme-dependent antibiotic resistance phenotype on the bacterium *E. coli*. In vitro studies reveal that heme binding to the integral fusion proteins occurs in a manner similar to that of cyt *b* to cause a major decrease in the level of nitrocefin hydrolysis without any apparent major changes to the structure of integral fusion proteins.

MATERIALS AND METHODS

Construction and Screening of the Domain Insert Library. The random insertion of a DNA cassette encoding cytochrome b_{562} (cyt *b*) into the *bla* gene encoding TEM β-lactamase was performed using a transposon-based approach described previously (*15*), except for the following additions. The original BLAΔ^{198} library comprising 198 variants with the engineered transposon MuDel (*31*) randomly inserted within the *bla* gene (*15*) was expanded to comprise 1644 additional variants. Removal of MuDel to generate the single random break in the *bla* gene and the subsequent insertion of cyt *b*-encoding DNA cassette were performed as described previously (*15*) to generate the domain insert library. The different DNA cassettes encoding the cyt *b* insert together with the nature of the linking sequences used to construct the library have also been described previously (*15*) and reproduced in Table S1 of the Supporting Information for the sake of clarity. To select TEM variants tolerant to insertion of cyt *b*, *E. coli* DH5α cells transformed with the domain insert library were plated on LB agar supplemented with 25 μg/mL ampicillin and incubated at 37 °C overnight. A total of 960 colonies that were capable of growth were used to inoculate 96-well culture plates containing LB medium supplemented with 25 μg/mL ampicillin. These new domain insert variants supplemented the original 112 clones isolated previously (*15*) and were screened for heme-dependent bacterial ampicillin resistance as described previously (*15*). *E. coli* DH5α cells containing the original parent vector that contains wild-type *bla* (pNOM) or a vector expressing separate wild-type *bla* and *cybC* genes encoding cyt *b* [pPB10 (*32*)] were used as controls.

Protein Overexpression and Purification. The gene encoding each individual cyt *b*−TEM fusion protein or wild-type TEM present within the pNOM plasmid used for the selection process was transferred without its signal sequence to pET42a in frame with a C-terminal hexahistidine affinity tag, as outlined in detail in the Supporting Information. Protein overexpression was performed using *E. coli* BL21(DE3) freshly transformed with the appropriate expression vector. Starter cultures were established in M9 minimal medium supplemented with 25 μg/mL kanamycin and were grown aerobically at 20 °C overnight. The starter cultures were used to inoculate 500 mL cultures of M9 medium also supplemented with 25 μg/mL kanamycin. The cultures were then grown at 20 °C until the OD_{600} reached 0.4. Overexpression was induced by the addition of 1 mM IPTG at 20 °C, and the cultures were incubated for up to ~60 h. The cells were then harvested and lysed using a French press.

After clarification of the cell lysate by centrifugation, each of the fusion proteins was predominantly recovered in the supernatant, showing the proteins to have been expressed in a soluble conformation. The supernatant was applied to a HisTrap HP column (GE Healthcare, 5 mL bed volume) that had been equilibrated with 10 mM Tris-HCl (pH 8) and 500 mM NaCl, and the column was washed to remove unbound protein. The hexahistine-tagged proteins were eluted using a linear gradient from 0 to 250 mM imidazole (Fisher Chemicals) in 10 mM

Table 1: Variants Conferring Heme-Dependent Ampicillin Resistance

Amino acid(s) replaced [a]	Variant number	Secondary structure [b]	Fusion protein [c]	Amp MIC (μg/ml)		
				No haem	10 μM Haem	Fold change [d]
n/a	pNOM[e]	-	-	40960	40960	0
n/a	pPB10[e]	-	-	40960	40960	0
n/a	DH5α[e]	-	-	<8	<8	0
P27Δ	Tc10[e]	H1	TEM_{26}-**GGS**-ADL-cytb-YR-**GGS**-$_{28}$TEM	32768	32768	0
G196Δ	Tc-3[e]	LP H8-H9	TEM_{195}-ADL-cytb-YS-$_{197}$TEM	32768	4096	8
L199P, T200Δ	Tc898		TEM_{199}-ADL-cytb-YR-**GGP**-$_{201}$TEM	32768	4096	8
A213Δ	Tc297	LP H9-H10	TEM_{212}-**GGS**-DL-cytb-YR-**GGS**-$_{214}$TEM	32768	1024	32
A213G, D214Δ	Tc68	LP H9-H10	TEM_{213}-DL-cytb-YR-**DH**-$_{215}$TEM	16384	128	128
A213G, D214Δ	Tc29[e]	LP H9-H10	TEM_{213}-**V**-DL-cytb-YR-**N**-$_{215}$TEM	16384	128	128
D214Δ	Tc945	LP H9-H10	TEM_{213}-ADL-cytb-YR-**GGN**-$_{215}$TEM	4096	128	32
A217G-G218Δ	Tc-28[e]	LP H9-H10	TEM_{217}-**S**-DL-cytb-YR-**PR**-$_{219}$TEM	16384	4096	4
P226R, A227Δ	Tc30[e]	LP H10-S3	TEM_{226}-**G**-DL-cytb-YR-**T**-$_{228}$TEM	16384	1024	16
S258Δ	Tc60	LP S4-S5	TEM_{257}-DL-cytb-YR-**C**-$_{259}$TEM	8192	128	64
T265M-T266Δ	Tc-22[e]	S5	TEM_{265}-**M**-DL-cytb-YR-**GA**-$_{267}$TEM	4096	512	8
M272I, D273Δ	Tc77	H11	TEM_{272}-**K**-DL-cytb-YR-**H**-$_{274}$TEM	32768	2048	16
M272Δ	Tc92	LP H10-H11	TEM_{271}-DL-cytb-YR-**S**-$_{273}$TEM	16384	128	128
D273Δ	Tc31[e]	H11	TEM_{272}-DL-cytb-YR-**H**-$_{274}$TEM	8192	512	32

[a]Residue numbering according to Ambler (*43*). Δ signifies residue deleted. [b]Secondary structure assignments according to Jelsch et al. (*44*). LP signifies loop. [c]Linker sequences are shown in bold and underlined. The sequence segment representing cyt *b* is colored red. Only terminal cyt *b* residues are shown, with the intervening sequence indicated by cyt *b*. [d]The *x*-fold change was calculated by dividing the ampicillin minimum inhibitory concentration value in the absence of heme by the value in the presence of heme (*15*). [e]Previously reported by Edwards et al. (*15*).

Tris-HCl (pH 8) and 500 mM NaCl. Eluate fractions containing TEM or the cyt *b*−TEM fusion protein were identified by SDS−PAGE and pooled and dialyzed against 10 mM sodium phosphate (pH 7).

The protein concentration was estimated from the absorbance at 280 nm, using a molar extinction coefficient of 30940 M^{-1} cm^{-1} for the cyt *b*−TEM fusion proteins or 27960 M^{-1} cm^{-1} for wild-type TEM. The molar extinction coefficients were calculated using the ExPASY server (*33*). As none of the fusion proteins caused the replacement of an aromatic amino acid with the cyt *b* domain and none of them contained aromatic residues in the linker regions, the same extinction coefficient was used for all of the fusion proteins. The heme concentration was determined as described previously (*15*).

Enzymatic Characterization of Protein Variants. Nitrocefin hydrolysis assays were conducted in reaction buffer [10 mM sodium phosphate (pH 7), 100 mM NaCl, and 1 mM potassium nitrate] at 25 °C. Enzyme kinetics were measured using 50 nM integral fusion protein or 5 nM Tc10 or TEM. The reaction was initiated by addition of nitrocefin (Becton-Dickinson) to the appropriate final concentration (2−200 μM) and the reaction followed by monitoring changes in absorbance at 485 nm (extinction coefficient of 14060 M^{-1} cm^{-1}) using a Hewlett-Packard 8452A spectrophotometer. Kinetic parameters were calculated using the initial rate of hydrolysis at each substrate concentration and curve fitting the data to the Michaelis−Menten equation. Curve fitting was conducted using KaleidaGraph (Synergy Software).

To analyze the effect of heme on nitrocefin hydrolysis, integral fusion protein samples were prepared at a concentration of 1 μM with heme concentrations ranging from 0 to 5 μM. As heme (Fluka) was dissolved in 0.5 M NaOH, all reaction mixtures were supplemented with additional NaOH to maintain a final NaOH concentration in the assay of 25 μM. Proteins were incubated with heme in the dark for ∼30 min to ensure heme binding had reached equilibrium, which were then diluted 100-fold into assay buffer [10 mM sodium phosphate (pH 7), 100 mM NaCl, and 1 mM potassium nitrate]. Reactions were initiated by addition of nitrocefin to a concentration of 100 μM, and the progress of the reaction was followed by monitoring changes in the absorbance at 485 nm as before. The effect of heme on the progress of the nitrocefin hydrolysis reaction by variant Tc29 was determined as follows. Hydrolysis was initiated by addition of 100 μM nitrocefin to the reaction mixture containing 50 nM protein. After 2 min, 12.5 μM NaOH, a molar equivalent of heme, or a 5-fold molar excess of heme was added to the cuvette.

Spectrophotometry. Absorbance spectra were recorded on a Cary 50 Bio spectrophotometer (Varian) using 10 μM protein in 10 mM sodium phosphate (pH 7) in the presence and absence of 10 μM heme. Oxidizing conditions were maintained by including 1 mM potassium nitrate in the sample, and reducing conditions were induced by the addition of 1 mM ascorbic acid. The absorbance spectrum of holo-Tc30 under oxidizing conditions was deconvoluted by subtraction of the free heme spectrum.

Circular Dichroism Spectroscopy. CD spectra were recorded on a Chirascan spectropolarimeter (Applied Photophysics) using a 1 mm quartz cuvette containing 10 μM protein in 10 mM sodium phosphate (pH 7) in either the presence or absence of 10 μM heme. Spectra were recorded from 185 to 260 nm at 1 nm resolution and with a bandwidth of 1 nm. Ellipticity readings (θ) were converted to extinction coefficients according to the formula $\Delta\varepsilon = \theta/(32980cl)$, where c is the concentration of peptide bonds (in molar) and l is the path length (in centimeters).

Size Exclusion Chromatography. SEC was performed using a Superdex 200 10/300 GL column (GE Healthcare) equilibrated with buffer comprised of 10 mM sodium phosphate (pH 7) and 100 mM NaCl. The fusion proteins were applied to the column as a 100 μL aliquot of ∼10 μM, and protein elution was followed by monitoring the absorbance of the eluate at 280 and 420 nm. The apparent molecular mass of each protein was determined from a calibration curve in which log(molecular mass) was plotted against K_{av} for the protein standards ribonuclease A (18.4 kDa), α-chymotrypsinogen (23 kDa), ovalbumin (39 kDa), albumin (65 kDa), transferrin (81 kDa), and γ-globulin (155 kDa). Blue dextran was used to determine the void volume of the column (V_0) and 1% acetone to determine the total volume (V_t).

RESULTS

Insertion of cyt b within TEM. Using the transposon-based random domain insertion approach (*15*) to link the activities of cyt *b* and TEM, a number of integral fusion proteins that conferred a major decrease in bacterial resistance to ampicillin in the presence of heme were found (Table 1). The transposon-based method essentially deletes a single residue (*31*) and replaces it with a new protein fragment/domain encoded in a DNA cassette (*15*). The nature of the method allows the user to determine the nature of residues that link the two proteins. Flexible defined tripeptide (GlyGlySer) or single randomized residues were used to construct the domain insert library. The method included the sampling of linking sequences at one join point, both points, or neither point [Table S1 of the Supporting Information (*15*)].

The presence of heme in the growth medium had a significant effect on the ability of a number of variants to confer an ampicillin resistance phenotype on *E. coli* (Table 1). The decrease in the minimum inhibitory concentration (MIC) of ampicillin that prevented cell growth due to the presence of heme depended on the variant and ranged from 4−8-fold (e.g., Tc3 and Tc28) to 128-fold (e.g., Tc29 and Tc92). The presence of heme in the growth medium had no effect on the MIC of ampicillin for cells expressing TEM alone or TEM and cyt *b* as individual proteins [Table 1 (*15*)].

The sites of cyt *b* insertion were located at different positions with respect to the three-dimensional structure of TEM but were generally concentrated in the C-terminal region of the β-lactamase (Figure 2). The majority of variants displaying switching behavior had no linker (e.g., Tc3) or short linkers at one (e.g., Tc92) or both (e.g., Tc77) connection points (Table 1). Tc297 was the only variant to contain the flexible GGS linker at both connection points. Insertion of cyt *b* occurred mainly in short loops within TEM comprised of five to eight residues. However, some were observed to occur in organized secondary structure: toward the end of helix 11 (Tc31 and Tc77) or strand S5 (e.g., Tc22). Many of the variants contained cyt *b* insertions at similar positions within TEM (e.g., A213-D214 and M272-D273), but with the in vivo switching magnitude dependent on the nature of the linker (Table 1). These positions may represent hot spots within TEM for communicating conformational events to the catalytic center of the enzyme. These insertion positions vary with respect to the active site. For example, A213 and D214 are ~12 Å immediately below the active site serine (S70) and abut residues critical to formation of the hydrogen bonding network at the heart of the active site (*30*) (vide infra). The M272-D273 site lies farther away (~18 Å) from S70 and abuts additional residues known to contribute to catalysis (vide infra). In both these cases and with other insertion positions (G128 and T266), cyt *b* is inserted in second-shell positions rather than directly into the active site. Other insertion positions (e.g., G196, T200, A227, and S257) lie on the opposite face of TEM, distant from the active site.

Enzymatic Analysis of Selected cyt b−TEM Integral Fusion Proteins. Four of the integral fusion proteins, Tc29, Tc30, Tc31, and Tc60 (see Figure 2 for relative insertion positions within TEM), that conferred a variety of changes in ampicillin MIC in the presence of heme ranging from 16- to 128-fold (Table 1) were chosen for more detailed analysis. They also represented insertion positions that were relatively close or distant from the active site (Figure 2B). As a control, a nonswitching variant was selected from the original domain insertion library and is termed Tc10 [insertion in place of Pro27 (Table 1 and Figure 2)]. Tc10 is essentially a "head-to-tail" fusion with a single covalent link between cyt *b* and TEM as signal sequence cleavage occurs between residues 25 and 26 of TEM. It is therefore unsurprising that the in vivo activity of this protein was unaffected by the presence of heme.

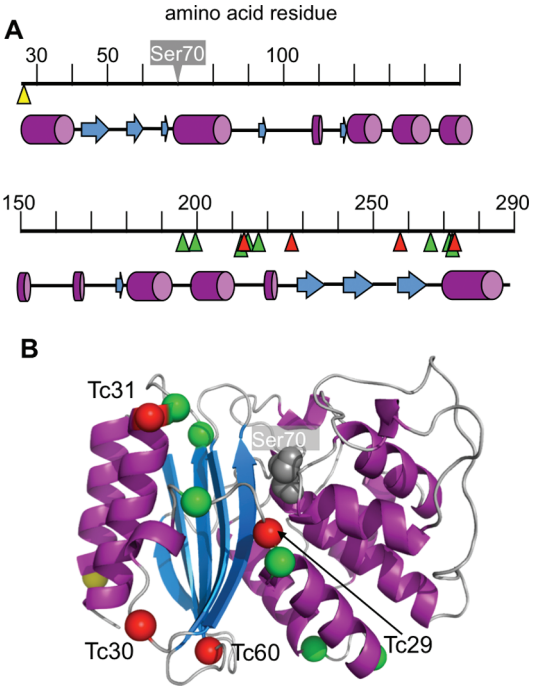

FIGURE 2: Tolerance of insertion of cyt *b* within TEM. (A) Representation of the primary structure of mature TEM showing the relative insertion positions of the cyt *b* domain that confer a heme-sensitive antibiotic resistance phenotype on *E. coli*. Further details concerning these variants can be found in Table 1. The active site serine (Ser70) is shown for reference. Red arrowheads indicate the positions of the residue deleted from TEM upon insertion of cyt *b* for variants analyzed in detail in this paper, and green arrowheads denote additional positions observed to reduce bacterial tolerance to ampicillin in the presence of heme. The yellow arrowhead denotes the cyt *b* insertion position of variant Tc10. The secondary structure of TEM as described by Jelsch et al. (*26*) is shown for reference. Purple cylinder for helix and blue arrow for strand. (B) Site of cyt *b* insertion with respect to the three-dimensional structure of TEM β-lactamase [PDB entry 1btl (*44*)]. Red, green, and yellow spheres correspond to the red, green, and yellow arrows, respectively, in panel A. The side chain of the active site Ser70 residue is shown as space-filled and colored gray.

Table 2: Enzymatic Properties of Integral Fusion Properties

	K_M (μM)	k_{cat} (s^{-1})	k_{cat}/K_M (s^{-1} μM^{-1})	switching magnitude[a]
TEM	26 ± 0.6	209 ± 44	8.0	1.2
Tc10	46 ± 6	187 ± 72	4.0	1.3
Tc29	60 ± 5	2.6 ± 0.6	0.04	> 80[b]
Tc30	45 ± 19	7.5 ± 2	0.16	7
Tc31	41 ± 1	1.1 ± 0.2	0.03	3
Tc60	113 ± 10	0.10 ± 0.01	0.001	7

[a]The *x*-fold change in nitrocefin hydrolysis in the presence of a 5-fold molar excess of heme. [b]Nitrocefin hydrolysis in the presence of heme was too slow to accurately determine the rate.

The enzyme kinetics of the apo forms for each cyt *b*−TEM hybrid were determined using the chromogenic β-lactam substrate nitrocefin (Table 2). As expected, the head-to-tail fusion,

Tc10, displayed enzyme kinetics similar to those of TEM, with only small differences in k_{cat} and K_M observed. By contrast, the level of nitrocefin hydrolysis by the cyt *b*−TEM integral fusions was markedly reduced, suggesting that insertion of cyt *b* within TEM has had a significant effect on the active site structure of the β-lactamase. The main effect of the insertion of the cyt *b* domain into TEM was a reduction (up to 3 orders of magnitude) in k_{cat} for each integral fusion protein. The observed K_M values for the integral fusion proteins were closer to those for TEM and Tc10, suggesting that the domain insertion has a weaker effect on substrate binding and that the reduction in the efficiency of these proteins is primarily mediated through changes to catalysis.

The direct effect of heme on the β-lactamase activity of each integral fusion protein was investigated in vitro using the purified proteins. As shown in Table 2 and Figure S1 of the Supporting Information, heme had little effect on the ability of TEM or Tc10 to hydrolyze nitrocefin. However, heme had a significant effect on the rate of nitrocefin hydrolysis for the integral fusion proteins that conferred heme-dependent ampicillin resistance on *E. coli* (Table 2). Addition of a molar equivalent of heme to Tc29 reduced the rate of nitrocefin hydrolysis by just more than 50%, and in the presence of a 5-fold molar excess of heme, less than 2% of the β-lactamase activity remained (Figure 3A). Tc30 exhibited heme-dependent nitrocefin hydrolysis similar to that of Tc29 (Figure 3B), except that just less than 15% of the activity remained in the presence of a 5-fold molar excess of heme (Table 2). Similar results were observed for variant Tc60, even though its enzymatic activity was the lowest of all the integral fusion variants (Figure S2 of the Supporting Information). The exception was Tc31, in which the β-lactamase activity increased slightly (~1.5-fold) in the presence of a molar equivalent of heme but decreased in the presence of an excess of heme (Figure S2 of the Supporting Information). The activity of the integral fusions was too low in the presence of heme for the reliable determination of kinetic parameters.

For all integral fusion variants, the magnitude of switching observed in vitro mirrored those observed in vivo (Tables 1 and 2), with the largest switcher in vivo, Tc29, also displaying the largest switching effect in vitro. Moreover, in the case of Tc29, the almost complete loss of activity in the presence of excess heme makes an accurate determination of the switching magnitude difficult. Conversely, Tc30 that conferred the smallest in vivo fold switch also displayed a smaller heme-dependent change in nitrocefin hydrolysis. It should be noted that in vivo measurements of the switching magnitude were taken using ampicillin as a substrate, while the in vitro measurements were taken using nitrocefin. This cephalosporin has a different general structure and is larger than the pencillin β-lactam, ampicillin, used in the original library selection. However, it is still a reasonable substrate for TEM. The preference of the enzyme for one substrate over the other could conceivably lead to differences in the magnitude of switching measured for each substrate, which has been observed previously with other engineered integral fusion proteins involving TEM (*34*).

A rapid response to an effector ligand is an important property of a protein switch. This property is not always present in engineered switching proteins, but when present, it facilitates the use of the protein for real-time measurements of ligand concentration or for rapid control of a synthetic reaction pathway in response to the change in the concentration of the allosteric ligand. To assess this response, the change in the rate of nitrocefin hydrolysis by variant Tc29 upon addition of heme after initiation of the reaction was investigated. The change in the rate of nitrocefin hydrolysis was essentially immediate, with the extent of the decrease in rate depending on the amount of heme added (Figure 3C).

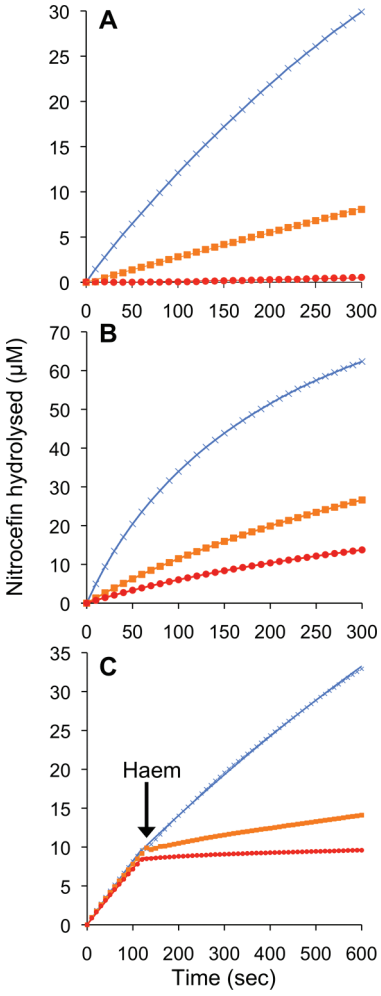

FIGURE 3: Heme-dependent enzymatic properties. The effect of heme on nitrocefin hydrolysis by (A) Tc29 and (B) Tc30 in the absence (blue crosses) or presence of 1:1 (orange squares) or 5:1 (red circles) heme:protein equivalent ratios. (C) Influence of heme on the progress of nitrocefin hydrolysis by Tc29. Nitrocefin hydrolysis was initiated as outlined in Materials and Methods, and after 2 min (indicated by the arrow), 12.5 μM NaOH (blue crosses), 1 molar equiv of heme (orange squares), or a 5-fold molar excess of heme (red circles) was added to the cuvette.

Heme Binding to cyt b−TEM Integral Fusion Proteins. The change in nitrocefin hydrolysis in the presence and absence of heme clearly demonstrates that heme is regulating β-lactamase activity in each switching protein, albeit to different extents. To confirm heme as an allosteric effector, it is necessary to demonstrate that heme binds to the inserted cyt *b* domain to mediate this effect. Heme binding to wild-type (wt) cyt *b* induces a characteristic absorbance spectrum; a strong absorbance peak at 419 nm and a small, broad peak at 530 nm are observed for holo-cyt *b* under oxidizing conditions, while under reducing conditions, the major peak red shifts to 427 nm and smaller distinctive peaks appear at 562 and 531 nm (*28*). Absorbance spectra of the variants were largely similar to those of wt cyt *b* (Figure 4 and Figure S3 of the Supporting Information), with only minor changes (1−3 nm) in λ_{max}, implying that the heme moiety is binding in a similar manner to the integral fusion proteins. However, some of the integral fusion variants had spectral

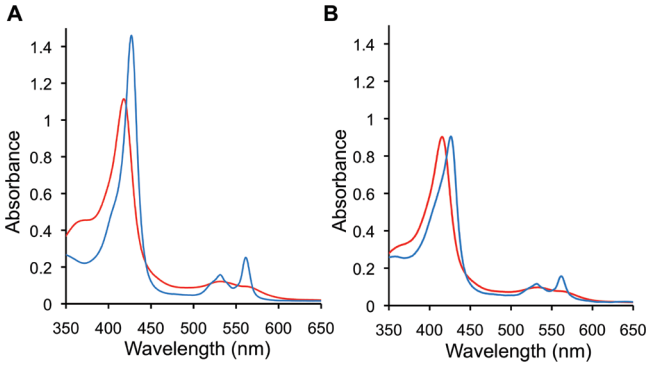

FIGURE 4: Heme binding characteristics of cyt *b*−TEM fusion proteins. Absorbance spectra of holo (A) Tc10 and (B) Tc29 under oxidizing (red line) and reducing (blue line) conditions. Absorbance spectroscopy was performed using equimolar amounts of heme and protein (10 μM) under both reducing and oxidizing conditions as outlined in Materials and Methods. Heme binding characteristics of Tc30 and Tc31 are shown in Figure S3 of the Supporting Information.

features that differed from those observed for wt cyt *b* and the head-to-tail variant Tc10. The intensities of the major peaks at 416 and 427 nm for Tc29 under oxidizing and reducing conditions, respectively, were similar (Figure 4B) despite a 1.5-fold higher extinction coefficient for the reduced wt holo-cyt *b* and the higher affinity of reduced versus oxidized heme (*28*). The peak at 419 nm for Tc30 under oxidizing conditions was much lower than expected and could only be observed upon subtraction of the free heme signal (Figure S3A of the Supporting Information). These results for Tc29 and Tc30 suggest that either the extinction coefficient has been significantly affected upon insertion of cyt *b* at these positions in TEM or the affinity of heme for the cyt *b* domain, especially in the case of Tc30, has been affected.

Structural Changes to Integral Fusion Proteins upon Heme Binding. To investigate the influence of heme on the structure of integral fusion proteins, we recorded the far-UV CD spectra of the selected integral fusion proteins in the presence and absence of heme (Figure 5A and Figure S4 of the Supporting Information). The general CD spectra of the apo forms of Tc29 and Tc31 suggest that cyt *b* has been incorporated into TEM to form a folded protein. The helical signals, as indicated by the troughs around 208 and 222 nm, for Tc31 particularly were significantly stronger than that of TEM alone (Figure S4B of the Supporting Information) and were similar in intensity to that of the head-to-tail fusion Tc10 (Figure 5A). Deconvolution of the CD spectra confirms that the helical content of Tc10 and Tc31 increases by approximately 15%, which is likely to be contributed by the cyt *b* insert. The helical signal associated with Tc29 was weaker than that observed for Tc10 but still stronger than that for TEM (Figure 5A). The CD spectrum for apo-Tc30, however, gave a helical signature weaker than that observed for TEM alone (Figure S3A of the Supporting Information), which suggests structure of this variant has been significantly affected by cyt *b* insertion.

Upon addition of heme, no obvious differences were observed (Figure 5A and Figure S4 of the Supporting Information) despite the fact that the cytochrome becomes more helical on binding heme. Although CD spectroscopy cannot analyze the contributions of secondary structure from specific regions of the protein to the overall spectrum, this suggests that heme binding does not perturb the structure of integral fusions to any great extent. It remains a possibility that small reductions in the level of secondary structure of TEM could have been masked by

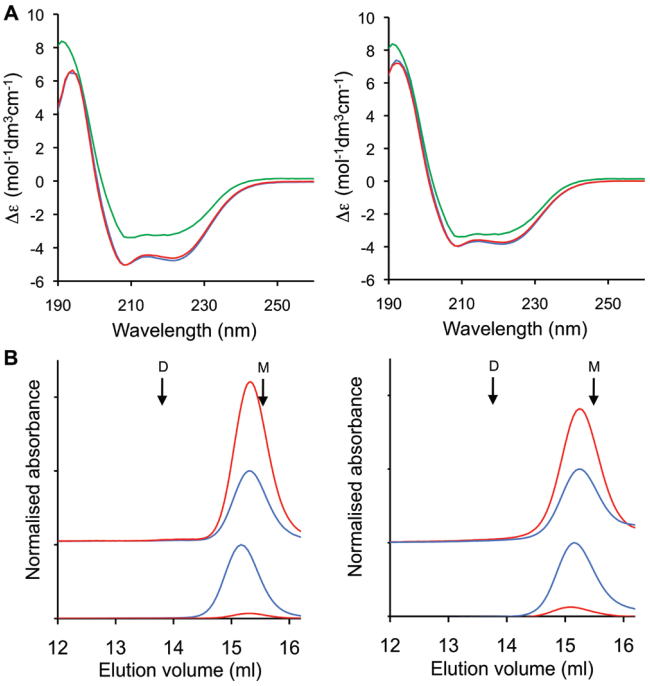

FIGURE 5: Structural changes to cyt *b*−TEM fusion proteins on heme binding. (A) Far-UV CD spectra of Tc10 (left) and Tc29 (right) in the presence (red line) and absence (blue line) of an equimolar concentration of heme. The CD spectrum of TEM (green line) is also shown for comparison. CD spectroscopy was performed using 10 μM protein in the presence or absence of 10 μM heme. (B) SEC elution profile of apo (bottom traces) and holo (top traces) forms of Tc10 (left) and Tc29 (right). The red and blue lines represent absorbance values at 420 and 280 nm, respectively. M and D refer to the theoretical elution points for the monomeric and dimeric forms, respectively. Size exclusion chromatography was performed with ~10 μM protein. The absorbance was normalized to 280 nm, with the peak intensity being 1.

corresponding increases in the level of helical structure of the cyt *b* domain. However, this is unlikely as proteins with cyt *b* insertions in three different positions within TEM, as well as Tc10, showed no real net change in the CD spectrum recorded in the presence of heme (Figure 5A and Figure S4 of the Supporting Information).

Size exclusion chromatography (SEC) was used to determine the apparent molecular mass and therefore oligomeric state of three switching variants: Tc29, Tc30, and Tc31. For all the integral fusion variants, both the apo- and holoproteins eluted at similar volumes (Figure 5B and Figure S5 of the Supporting Information) with an apparent molecular mass of ~45 kDa, close to the calculated monomeric mass of 41 kDa. The elution volumes were also essentially the same as that observed for the head-to-tail fusion variant Tc10 (Figure 5B). No peaks at elution volumes corresponding to the dimer or other higher-order structures were observed. Therefore, binding of heme to the switching integral fusion proteins does not appear to induce any significant changes in quaternary structure or induce aggregation.

DISCUSSION

The ability to take two unrelated proteins with useful individual properties, such as sensing and reporting functions, and link them in a manner in which their activities are coupled provides an opportunity to construct novel biomolecular components that act as molecular switches. Domain insertion (*7*, *9*)(Figure 1A) provides a generic approach for coupling the independent

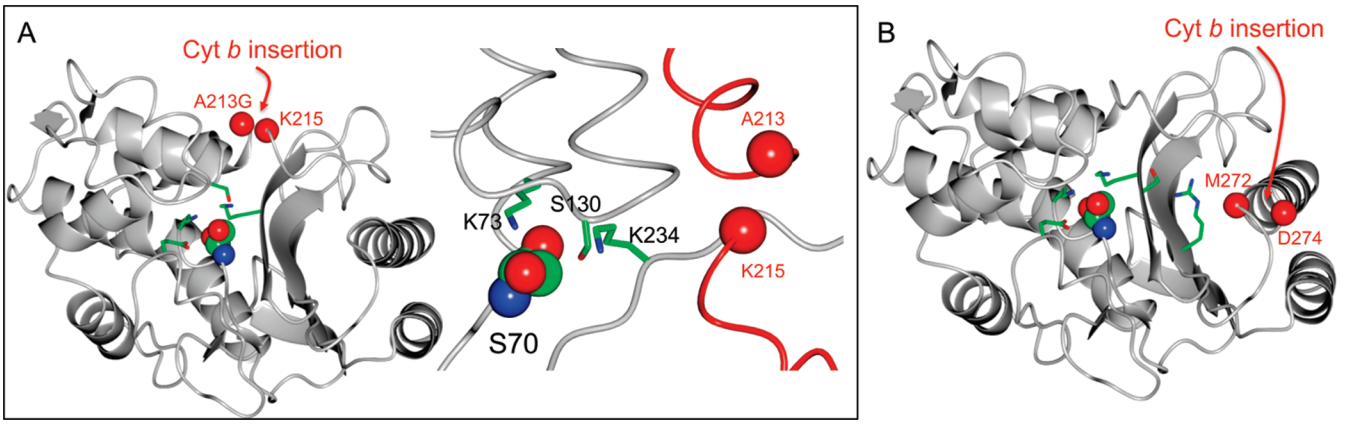

FIGURE 6: Insertion of cyt *b* in relation to the catalytic site of TEM for (A) Tc29 and (B) Tc31. The single red spheres correspond to the cyt *b* insertion site and are annotated on the diagrams. The active site serine, S70, is shown as a sphere, and other related catalytic residues are shown as cylinders. In A, the right panel is a magnified region of the left panel. Molecular structures were generated using CCP4mg (*45*).

activities of individual proteins to generate engineered, single-unit systems that can mimic the mechanism of allostery (*8*, *35*). However, domain insertion could be considered a largely destructive mutational process, especially to the protein accepting the insert due to a break in the continuity of the polypeptide chain. Furthermore, if a domain insertion is tolerated, there is no guarantee that the new chimeric protein will exhibit significant switching behavior. Given the current limitation of our ability to predict a tolerated insertion site within a target protein together with the nature of the linking sequence that results in a coupled binary protein system, a nonhomologous recombination-directed evolution strategy provides the ideal approach for generating and sampling the required sequence space to facilitate the construction of switching proteins. We demonstrate this here by introducing heme-dependent activity into the useful reporter protein TEM β-lactamase through the insertion of cyt *b*.

TEM has been used in the past as a protein being inserted into a variety of acceptor domains, but this has largely resulted in integral fusion proteins with generally low-magnitude switching characteristics (*12*, *36*, *37*) unless TEM is circularly permuted at sites closer to the active site than the naturally occurring N- and C-termini (*16*, *34*). By reversing this strategy and inserting the small heme binding protein cyt *b* into certain sites within TEM, we found β-lactamase activity became dependent on the presence of heme both in vivo (Table 1) and in vitro (Figure 3, Table 2, and Figure S2 of the Supporting Information). In all the variants presented here, negative regulation of β-lactamase activity on heme binding was observed. Negative allostery is not uncommon in nature and is exemplified by end product inhibition feedback in biosynthetic pathways (*6*). However, as heme binds noncovalently with affinity being influenced by various factors such as redox conditions (*28*), the switch is potentially reversible with condition-dependent heme dissociation leading to restoration of β-lactamase activity.

Generally, cyt *b*-TEM integral fusion variants that displayed switching properties contained inserts within loops or close to the end of organized secondary structure (Figure 2 and Table 1). Loops can readily adapt their conformation to accommodate changes as a result of mutation, including indel mutations that influence the polypeptide backbone as well as the side chain (*38*), thus are more likely to tolerate the insertion of an additional protein domain. Insertion within a helix or strand is likely to cause major disruption to local interactions critical to maintaining the integrity of these structural elements through register shifts and are consequently more likely to be deleterious. However, the nature of the loop and its relative positioning is critical. Most of the switching variants contain inserts within short (5−8 residues) loops. Insertions within longer loops such as that linking helices H3 and H4 are tolerated but no heme-dependent β-lactamase activity was observed (*15*). Furthermore, some loop regions that might be considered ideal for introducing switching into TEM, such as within the catalytically important Ω loop, have been observed to tolerate domain insertion but without the accompanying heme-dependent β-lactamase activity (*15*).

Many of the variants contained cyt *b* insertions at similar positions within TEM (e.g., A213-D214 and M272-D273) but with the *in vivo* switching magnitude dependent on the nature of the linker (Table 1); these sites may represent hotspots within TEM whereby conformational events can be efficiently communicated to the active center of the enzyme. Variant Tc29 with an observed switching magnitude of ~2 orders of magnitude (Tables 1 and 2) had cyt *b* inserted in the A213-D214 region. This second shell region abuts onto residues S130 and K234 that contribute to the hydrogen bond network of the active site of TEM (Figure 6A). Both S130 and K234 are known to be important for catalysis (*30*) thus insertion of cyt *b* close to these residues is likely to disrupt the hydrogen bond network and thus catalysis (as evidenced by the drop in k_{cat} by nearly 2 orders of magnitude; Table 2). However, it also provides an excellent insertion position by which to couple the activities of cyt *b* and TEM. The M272-D273 region can also be considered as a second shell site (Figure 6B) but is more remote (~18 Å) from the active site serine (S70) than the A213-D214 (~12 Å). Also, residues such as S235 and R244 that lie close to the D273 insertion point contribution to catalysis is a relatively minor (*30*) and may account for the lower switching capacity of Tc31 compared to Tc29. Furthermore, compared with the CD spectrum of the head-to-tail fusion variant Tc10, the structures of TEM and cyt *b* may be more integrated in variant Tc29 compared to Tc31 as the increase in the helical signature is much less (Figure 5A and Figure S4 of the Supporting Information). The CD spectrum for Tc31 is very similar to that of Tc10, suggesting that cyt *b* and TEM may still retain a high degree of structural independence. Therefore, true structural integration coupled with an insertion in a second-shell location may be pivotal for generation of high-magnitude switching variants.

Variants Tc30 and Tc60 contained cyt *b* inserted at positions on the face of TEM opposite that of the active site (Figure 2). It is

unclear how switching is achieved in these and other variants with cyt *b* inserted distant from the active site (e.g., Tc3 and Tc898), but it is likely to be achieved by propagation through a linked network of interactions (*14*). However, the observed switching magnitude for these variants is generally lower than that observed for the second-shell insertion variants (Tables 1 and 2). For variants Tc30 and Tc60, cyt *b* insertion is also very disruptive in terms of structure and function. Tc60 was the worst performer in terms of enzyme kinetics, with the catalytic efficiency (k_{cat}/K_M) decreasing nearly 4 orders of magnitude (Table 2), and was generally unstable. While Tc30 was the most catalytically efficient of all the integral fusion variants, both the general structure (Figure S4A of the Supporting Information) and heme binding affinity (Figure S3A of the Supporting Information) had been disrupted on cyt *b* insertion. This later observation implies that communication between the domains can in some instances be bidirectional, so that in addition to the cyt *b* domain affecting the activity of TEM, TEM is also able to influence the heme binding properties of cyt *b*. This is further exemplified by Tc29, in which the intensities of λ_{max} at 419 and 427 nm under oxidizing and reducing conditions, respectively, were similar despite a ~1.5-fold higher extinction coefficient for the reduced wt holo-cyt *b* and the normally higher affinity of cyt *b* for ferrous heme over the ferric form (*28*). Such influences on heme binding to cyt *b* are likely to be due to heme binding close to the N- and C-termini of cyt *b* (Figure 1B) and, therefore, the domain interface region in the integral fusion proteins.

Tc31 was the only variant to exhibit slightly enhanced β-lactamase activity (~1.5-fold) in the presence of heme but only up to equimolar concentrations of heme and protein; activity decreased upon addition of excess heme (Figure S2A of the Supporting Information and data not shown). This phenomenon was routinely observed for Tc31 and implies that heme is able to regulate this protein both positively and negatively depending on the concentration of heme. While this provides an interesting facet to the regulation of Tc31, we are unable to provide a clear explanation of how this phenomenon might arise.

The nature of the sequences that link cyt *b* and TEM also proved to be critical. In most cases, cyt *b*−TEM variants that exhibited heme-dependent β-lactamase activity had no or short linkers (Table 1). Cyt *b*−TEM chimeras with longer GGS-based linkers rarely displayed switching behavior even when cyt *b* was inserted at positions within TEM known to introduce heme-dependent β-lactamase activity (*15*). Traditional, longer (at least three residues), inherently flexible glycine-rich sequences have been used extensively to link domains, but this is likely to result in decoupling of the two activities. Short linkers as observed here and for another domain insert protein switch (*16*, *34*) could be essential to allow transfer of conformational events between the two active centers.

One mechanism postulated for communication in engineered integral protein fusion proteins occurs via gross changes to protein structure, whereby switching is achieved though events such as coupled folding and unfolding (*26*, *27*, *39*). This would be the most obvious explanation given that heme binding resulted in a reduction in activity in all the switching integral fusion proteins (Tables 1 and 2, Figure 3, and Figure S2 of the Supporting Information). However, in each case, there were no obvious changes in the CD spectra (Figure 5A and Figure S4 of the Supporting Information) or the apparent molecular mass (Figures 5B and Figure S5 of the Supporting Information), suggesting that there was no major change to the structure of the integral fusion proteins on heme binding. Although CD spectroscopy cannot analyze the contributions or fluctuations of the secondary structure from specific regions of the protein to the overall spectrum, this result indicates that heme binding resulted in no net change in the secondary structure content of each integral fusion protein. It remains a possibility that small reductions in the secondary structure of TEM could have been masked by corresponding increases in the level of helical structure of the cyt *b* domain. However, this is unlikely as proteins with cyt *b* insertions in three different positions within TEM, as well as Tc10, exhibited no net change in the CD spectrum recorded in the presence of heme. Furthermore, the formation of a disulfide bridge in TEM that links C77 in the core helix to C123 could act as a molecular bolt that prevents TEM from undergoing gross unfolding events in response to heme binding.

Given that coupled protein unfolding is unlikely to give rise to the negative regulation observed in the cyt *b*−TEM integral fusion proteins, more subtle structural effects that cannot be detected by the coarse analysis of CD spectroscopy and SEC may be responsible. One possible explanation is a phenomenon termed dynamic allostery (*40*−*42*). This is primarily an entropic effect in which binding of the allosteric ligand results in a local rigidification at the binding site, and this change in the dynamic flexibility of a region of the protein is communicated to the remote site through changes in van der Waals interactions. This would connect with the change in dynamics of the N- and C-terminal helices of cyt *b* on heme binding (*21*, *22*, *24*); in the absence of heme, the termini of cyt *b* are unstructured and dynamic but when heme binds become more structured and rigid, trapping TEM in an inactive state. The observation that gross structural changes are not a prerequisite for coupling the functions of unrelated proteins is important for the construction of artificial protein switches for use in synthetic biology. This will potentially allow the utilization of a wider range of sensing domains whereby the conformational change is subtle or limited to a change in inherent flexibility upon ligand binding.

It is apparent that insertion of cyt *b* had a detrimental effect on the TEM β-lactamase activity. Generally, the ampicillin MIC values were reduced compared to those of wt TEM, some as much as 10-fold (Table 1). This was mirrored in the enzyme kinetics for nitrocefin of the selected variants (Table 2), with k_{cat} particularly affected, decreasing by more than 30-fold. In comparison, K_M values for the cyt *b*−TEM integral fusion variants were similar to those of wt TEM and the head-to-tail fusion variant Tc10 (Table 1), suggesting that catalysis rather than substrate binding had been affected the most. As the selected variants had switching properties, it is not surprising that enzyme kinetics have been influenced dramatically as it suggests that the point of insertion is linked directly or indirectly to residues critical to catalysis, which has been described for Tc29 and Tc31 (Figure 6). The decrease in catalytic efficiency in this case may be a function of the use of cyt *b* as the sensing domain rather than the domain insert approach per se as other protein switches constructed by the domain insertion approach have respectable catalytic activities (*34*, *37*). Despite the apparent decrease in the catalytic efficiencies of the cyt *b*−TEM integral fusion proteins, TEM activity is still significant and can now be modulated by heme. These constructs could form the starting scaffold for further whole protein-directed evolution to optimize activity while maintaining heme-dependent activity.

In conclusion, we have demonstrated here that it is possible to construct artificial protein switches on the basis of the concept of

allostery using a directed evolution approach through linking the normally unrelated proteins cyt *b* and TEM β-lactamase by a strategy termed domain insertion. The observed link of heme and bacterial antibiotic resistance in vivo correlates with the in vitro heme-induced deactivation of TEM through the binding of heme to the domain-inserted cyt *b*. Communication between the heme binding and catalytic sites is thought to occur through subtle conformational changes rather than gross structural changes. This demonstrates that domain insertion coupled with directed evolution is a robust strategy for creating novel protein switches that have the potential to form key biomolecular components in the emerging area of synthetic biology and provide a novel route for probing the role of remote conformational events in regulating protein function.

SUPPORTING INFORMATION AVAILABLE

Supplementary methods, Table S1, and Figures S1−S5. This material is available free of charge via the Internet at http://pubs.acs.org.

REFERENCES

1. Channon, K., Bromley, E. H., and Woolfson, D. N. (2008) Synthetic biology through biomolecular design and engineering. *Curr. Opin. Struct. Biol. 18*, 491–498.
2. Koide, S. (2009) Generation of new protein functions by nonhomologous combinations and rearrangements of domains and modules. *Curr. Opin. Biotechnol. 20*, 398–404.
3. Lim, W. A. (2002) The modular logic of signaling proteins: Building allosteric switches from simple binding domains. *Curr. Opin. Struct. Biol. 12*, 61–68.
4. Goodey, N. M., and Benkovic, S. J. (2008) Allosteric regulation and catalysis emerge via a common route. *Nat. Chem. Biol. 4*, 474–482.
5. Changeux, J. P., and Edelstein, S. J. (2005) Allosteric mechanisms of signal transduction. *Science 308*, 1424–1428.
6. Lindsley, J. E., and Rutter, J. (2006) Whence cometh the allosterome? *Proc. Natl. Acad. Sci. U.S.A. 103*, 10533–10535.
7. Ferraz, R. M., Vera, A., Aris, A., and Villaverde, A. (2006) Insertional protein engineering for analytical molecular sensing. *Microb. Cell Fact. 5*, 15.
8. Fastrez, J. (2009) Engineering allosteric regulation into biological catalysts. *ChemBioChem 10*, 2824–2835.
9. Ostermeier, M. (2005) Engineering allosteric protein switches by domain insertion. *Protein Eng., Des. Sel. 18*, 359–364.
10. Krishna, M. M., and Englander, S. W. (2005) The N-terminal to C-terminal motif in protein folding and function. *Proc. Natl. Acad. Sci. U.S.A. 102*, 1053–1058.
11. Baird, G. S., Zacharias, D. A., and Tsien, R. Y. (1999) Circular permutation and receptor insertion within green fluorescent proteins. *Proc. Natl. Acad. Sci. U.S.A. 96*, 11241–11246.
12. Betton, J. M., Jacob, J. P., Hofnung, M., and Broome-Smith, J. K. (1997) Creating a bifunctional protein by insertion of β-lactamase into the maltodextrin-binding protein. *Nat. Biotechnol. 15*, 1276–1279.
13. Collinet, B., Herve, M., Pecorari, F., Minard, P., Eder, O., and Desmadril, M. (2000) Functionally accepted insertions of proteins within protein domains. *J. Biol. Chem. 275*, 17428–17433.
14. Lee, J., Natarajan, M., Nashine, V. C., Socolich, M., Vo, T., Russ, W. P., Benkovic, S. J., and Ranganathan, R. (2008) Surface sites for engineering allosteric control in proteins. *Science 322*, 438–442.
15. Edwards, W. R., Busse, K., Allemann, R. K., and Jones, D. D. (2008) Linking the functions of unrelated proteins using a novel directed evolution domain insertion method. *Nucleic Acids Res. 36*, e78.
16. Guntas, G., Mansell, T. J., Kim, J. R., and Ostermeier, M. (2005) Directed evolution of protein switches and their application to the creation of ligand-binding proteins. *Proc. Natl. Acad. Sci. U.S.A. 102*, 11224–11229.
17. Baldwin, A. J., Busse, K., Simm, A. M., and Jones, D. D. (2008) Expanded molecular diversity generation during directed evolution by trinucleotide exchange (TriNEx). *Nucleic Acids Res. 36*, e77.
18. Ponka, P. (1999) Cell biology of heme. *Am. J. Med. Sci. 318*, 241–256.
19. Reedy, C. J., and Gibney, B. R. (2004) Heme protein assemblies. *Chem. Rev. 104*, 617–649.
20. Rodgers, K. R. (1999) Heme-based sensors in biological systems. *Curr. Opin. Chem. Biol. 3*, 158–167.
21. Arnesano, F., Banci, L., Bertini, I., Faraone-Mennella, J., Rosato, A., Barker, P. D., and Fersht, A. R. (1999) The solution structure of oxidized *Escherichia coli* cytochrome b_{562}. *Biochemistry 38*, 8657–8670.
22. D'Amelio, N., Bonvin, A. M., Czisch, M., Barker, P., and Kaptein, R. (2002) The C terminus of apo-cytochrome b_{562} undergoes fast motions and slow exchange among ordered conformations resembling the folded state. *Biochemistry 41*, 5505–5514.
23. Faraone-Mennella, J., Gray, H. B., and Winkler, J. R. (2005) Early events in the folding of four-helix-bundle heme proteins. *Proc. Natl. Acad. Sci. U.S.A. 102*, 6315–6319.
24. Feng, Y., Sligar, S. G., and Wand, A. J. (1994) Solution structure of apo-cytochrome b_{562}. *Nat. Struct. Biol. 1*, 30–35.
25. Garcia, P., Bruix, M., Rico, M., Ciofi-Baffoni, S., Banci, L., Ramachandra Shastry, M. C., Roder, H., de Lumley Woodyear, T., Johnson, C. M., Fersht, A. R., and Barker, P. D. (2005) Effects of heme on the structure of the denatured state and folding kinetics of cytochrome b_{562}. *J. Mol. Biol. 346*, 331–344.
26. Jones, D. D., and Barker, P. D. (2004) Design and characterisation of an artificial DNA-binding cytochrome. *ChemBioChem 5*, 964–971.
27. Jones, D. D., and Barker, P. D. (2005) Controlling self-assembly by linking protein folding, DNA binding, and the redox chemistry of heme. *Angew. Chem., Int. Ed. 44*, 6337–6341.
28. Robinson, C. R., Liu, Y., Thomson, J. A., Sturtevant, J. M., and Sligar, S. G. (1997) Energetics of heme binding to native and denatured states of cytochrome b_{562}. *Biochemistry 36*, 16141–16146.
29. Springs, S. L., Bass, S. E., and McLendon, G. L. (2000) Cytochrome b_{562} variants: A library for examining redox potential evolution. *Biochemistry 39*, 6075–6082.
30. Matagne, A., Lamotte-Brasseur, J., and Frere, J. M. (1998) Catalytic properties of class A β-lactamases: Efficiency and diversity. *Biochem. J. 330* (Part 2), 581–598.
31. Jones, D. D. (2005) Triplet nucleotide removal at random positions in a target gene: The tolerance of TEM-1 β-lactamase to an amino acid deletion. *Nucleic Acids Res. 33*, e80.
32. Barker, P. D., Nerou, E. P., Freund, S. M., and Fearnley, I. M. (1995) Conversion of cytochrome b_{562} to c-type cytochromes. *Biochemistry 34*, 15191–15203.
33. Gasteiger, E., Gattiker, A., Hoogland, C., Ivanyi, I., Appel, R. D., and Bairoch, A. (2003) ExPASy: The proteomics server for in-depth protein knowledge and analysis. *Nucleic Acids Res. 31*, 3784–3788.
34. Guntas, G., Mitchell, S. F., and Ostermeier, M. (2004) A molecular switch created by in vitro recombination of nonhomologous genes. *Chem. Biol. 11*, 1483–1487.
35. Villaverde, A. (2003) Allosteric enzymes as biosensors for molecular diagnosis. *FEBS Lett. 554*, 169–172.
36. Doi, N., and Yanagawa, H. (1999) Design of generic biosensors based on green fluorescent proteins with allosteric sites by directed evolution. *FEBS Lett. 453*, 305–307.
37. Guntas, G., and Ostermeier, M. (2004) Creation of an allosteric enzyme by domain insertion. *J. Mol. Biol. 336*, 263–273.
38. Simm, A. M., Baldwin, A. J., Busse, K., and Jones, D. D. (2007) Investigating protein structural plasticity by surveying the consequence of an amino acid deletion from TEM-1 β-lactamase. *FEBS Lett. 581*, 3904–3908.
39. Radley, T. L., Markowska, A. I., Bettinger, B. T., Ha, J. H., and Loh, S. N. (2003) Allosteric switching by mutually exclusive folding of protein domains. *J. Mol. Biol. 332*, 529–536.
40. Cooper, A., and Dryden, D. T. F. (1984) Allostery without conformational change: A plausible model. *Eur. Biophys. J. 11*, 103–109.
41. Smock, R. G., and Gierasch, L. M. (2009) Sending signals dynamically. *Science 324*, 198–203.
42. Tzeng, S. R., and Kalodimos, C. G. (2009) Dynamic activation of an allosteric regulatory protein. *Nature 462*, 368–372.
43. Ambler, R. P., Coulson, A. F., Frere, J. M., Ghuysen, J. M., Joris, B., Forsman, M., Levesque, R. C., Tiraby, G., and Waley, S. G. (1991) A standard numbering scheme for the class A β-lactamases. *Biochem. J. 276* (Part 1), 269–270.
44. Jelsch, C., Mourey, L., Masson, J. M., and Samama, J. P. (1993) Crystal structure of *Escherichia coli* TEM1 β-lactamase at 1.8 Å resolution. *Proteins 16*, 364–383.
45. Potterton, L., McNicholas, S., Krissinel, E., Gruber, J., Cowtan, K., Emsley, P., Murshudov, G. N., Cohen, S., Perrakis, A., and Noble, M. (2004) Developments in the CCP4 molecular-graphics project. *Acta Crystallogr. D60*, 2288–2294.